RESEARCH ARTICLE OPEN ACCESS

Evaluation of Volumetric Concentration of Ferrofluid Useful For Heat Extraction in High Power Transformers

Sanjay Kemkar*, Milind Vaidya**, Sanjana Kemkar***, Megha Chaple****, Sanika Dusane*****, Siddhesh Thorat******, Madhu Bagul*******, Sanjukta Kemkar********, Rajeshwari Thorat*********, Shital Sabale**********

**(Department of Physics, Smt. CHM, Ulhasnagar, India)*
***(Department of Physics, Vedanta College, Vitthalwadi, India)*
****(Smolensk State Medical University, Smolensk, Russia)*
*****(Department of Electrical Engineering, LTCE, Navi Mumbai, India)*
******(Department of Electrical Engineering, LTCE, Navi Mumbai, University of Mumbai, India)*
*******(Department of Electrical Engineering, LTCE, Navi Mumbai, University of Mumbai, India)*
********(Department of Electrical Engineering, LTCE, Navi Mumbai, University of Mumbai, India)*
*********(Department of Chemistry, Smt. CHM, Ulhasnagar, University of Mumbai, India)*
**********(Department of Electrical Engineering, LTCE, Navi Mumbai, University of Mumbai, India)*
***********(Chemist, Delphi Powers Ent, Mumbai, India)*
Corresponding Auther : Sanjay Kemkar

ABSTRACT
In conventional method, transformer oil is used as a coolant under natural convection. Transformer oils have low cooling efficiency due to low thermal conductivity. This work proposes the use of ferrofluid with transformer oil as a hydrocarbon carrier and evaluation of volumetric concentration thereof. Ferrofluid is a super-paramagnetic fluid and is used as a coolant. This enhances heat extraction from high power transformers. Addition of magnetic nanoparticles in transformer oil treated with a suitable stabilizer enhances the thermal conductivity of mixed solution and cooling efficiency thereafter. It also increases the dielectric strength of transformer oil. This thermal property of ferrofluid changes with volumetric concentration as well as diameter of magnetic nano particles. Therefore evaluation of volumetric concentration is important to make sure proper ferrofluid is used in electrical devices such as high power transformers.

Keywords - Ferrofluid, Volumetric Concentration, Transformer, Thermal conductivity, Transformer Oil, Heat Extraction

---

Date of Submission: 08-06-2018 Date of acceptance:23-06-2018

I. INTRODUCTION

Ferrofluid is a suspension of Nano-sized magnetic particles in a hydrocarbon carrier liquid [19]. We have synthesized Fe_3O_4 nano particles by chemical co-precipitation method. This is bottom up approach in making nano particles. These particles are ferrimagnetic in nature. The ferrofluids have been used in various applications. Some applications in the field of fiber optics [17], tilt angle measurement [18], voice coil in speaker [2] are very promising. Temperature sensitivity issue has already been studied. Attempts have also been carried out in generating small amount of energy [1]. Usually a strong magnetic field exists around the windings of the transformer due to high currents. In general, cooling of the transformer windings i.e. primary and secondaries and the core is achieved by natural convection by air or with the use of transformer oil. Hence the window area filled with the heat carrier should have higher dimensions for high power transformers. With the use of ferrofluid in transformer oil, heat transfer is improved. The magnetization of the ferrofluid decreases with increase in temperature. The heat transfer is caused due to the circulation of ferrofluid due to the magnetic field around the winding of the transformer. Ferrofluid accelerates the cooling by its magnetic properties and causes forced cooling [3].

It is also observed that, for a specific range of volumetric concentration of magnetic nanoparticles in the fluid, the dielectric strength of transformer oil increases to about three times higher than that of transformer oil and was studied elsewhere. When an external magnetic field is further applied to the ferrofluid, the dielectric breakdown strength increases to about 40% of the pure transformer oil [4]. Previous experimental investigations have demonstrated that, for lower

temperatures the saturation magnetization is high [5].

In Fe_3O_4 based transformer oil, the polarized and higher permittivity suspended particles are attracted towards the high stress areas of the transformer, thus providing better insulating efficiency in external magnetic field [6]. During the AC dielectric breakdown of magnetic fluid based transformer oil, luminous and audible discharges were observed long before the complete breakdown of the oil [7].

Many researchers have also studied the application of thermal conductivity for the enhancement of efficient transfer of heat in the field of thermo-magnetics. Previous studies have shown that the thermal conductivity increases with the increase in volume concentration of the ferrofluids. Also, for smaller sized particles, the thermal conductivity is observed to be higher [8]. It is a known fact that, with an increase in temperature, the ratio of thermal conductivity of aqueous, non-aqueous nano fluids and the base fluid remains constant as well as the viscosity ratio also remains constant. Also, experimental investigations have proved that the DC conductivity of the ferrofluid varies with varying volumetric concentration [16].

To achieve the better results on transformer cooling, it is very important to use the ferrofluid with higher volumetric concentration. Ferrofluid with lower sized particles are more suitable for transformer cooling. The key point in extraction of heat from high power transformer is thermal conductivity of coolant. Analysis of effect of variation in volumetric concentration and particle size is presented here. The diameters of nano particles prepared are about 12nm, 13nm, 24nm and 30nm. If there is no proper cooling in high power transformer, it will operate in derated condition. This situation is unwarranted and may turn into dangerous one. Therefore, it is proper to keep in check the volumetric concentration of the ferrofluid before its application in the transformer oil. Thus, the evaluation of volumetric concentration of ferrofluid plays a significant role on the efficiency of the transformer.

II. PREPARATION OF FERROFLUIDS

Magnetite (Fe_3O_4) is widely used as magnetic nanoparticle. Fe_3O_4 is formed as a co-precipitate when $FeCl_2$ and $FeCl_3$ are mixed with alkaline solution. After removing the salt residue by cleaning with de-ionised water, Fe_3O_4 particles were obtained which were then coated with a fatty acid which acts as a surfactant. Homogenous magnetic fluid was prepared using transformer oil as a carrier fluid. The study of variation of surface tension with respect to the volumetric concentration of the ferrofluid was carried out elsewhere. The observations for four different values of volumetric concentrations were taken and a graph was plotted between the surface tension and volumetric concentration. The results show an increase in the surface tension with increase in the volumetric concentration of the ferrofluid [9].

2.1 Importance of Soret effect observed in ferrofluid

In mixtures having mobile particles, an effect called Soret effect is observed due to a phenomenon called thermophoresis. It is observed when a mixture having a thermal gradient is subjected to an externally applied static uniform magnetic field. In this effect, the molecules of the solute and the solvent are thermally diffused, and it is characterized by Soret Coefficient (S_T). The nanoparticles are forced to travel in a direction perpendicular to the applied magnetic field. The Soret Coefficient is considered to be negative, when the particles tend to accumulate in the region of high temperatures ($S_T < 0$), and considered to be positive when the particles tend to traverse to the region of low temperatures ($S_T > 0$) [1]. It is also observed that Soret Coefficient is a function of the volumetric concentration. As a result, Soret effect aids the heat extraction process by inducing forced circulation of nanoparticles from higher temperature regions near the transformer windings to the relatively lower temperature regions near the walls of the transformer tank, thus promoting better cooling efficiency [10,11]. An increase in the thermal conductivity was observed when the heat flux and magnetic field were aligned parallel; while it decreased when the heat flux and magnetic field were aligned in a perpendicular manner [12].

According to existing theories, when ferrite or ferromagnetic nano particles are dispersed in a carrier fluid, the thermal conductivity of the fluid increases drastically than pure hydrocarbon carrier. The temperature gradient of the surface layer of spherical nanoparticles is notably lesser than that in the carrier liquid [13-15].

III. CHARACTERIZATION OF Fe_3O_4 NANOPARTICLES

The TEM of Fe_3O_4 samples were obtained and shown in Fig.3.1, Fig.3.2, Fig.3.3 and Fig.3.4 having sizes of the nanoparticles of 30nm, 24nm, 19nm, 13nm prepared at 8 pH, 10 pH, 11.5 pH and 12.5 pH respectively.

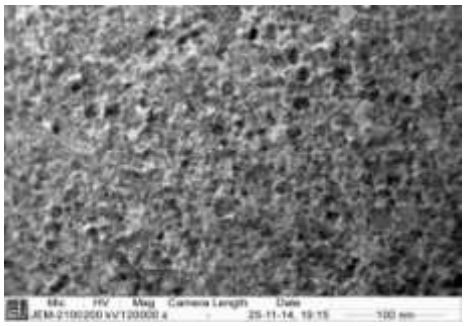

Fig.3.1: TEM image of nanoparticle of 30nm prepared at 8 pH.

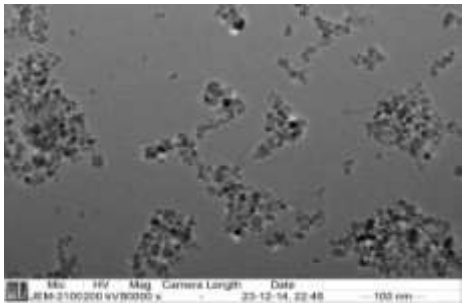

Fig.3.2: TEM image of nanoparticle of 24nm prepared at 10 pH.

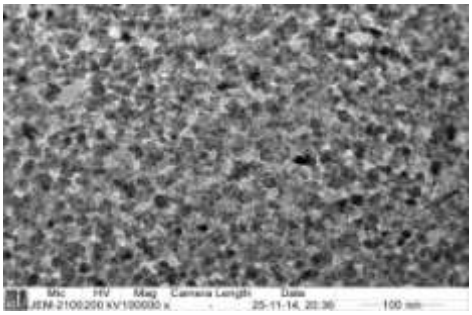

Fig.3.3: TEM image of nanoparticle of 19nm prepared at 11.5 pH.

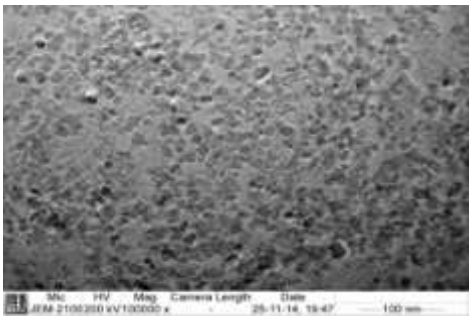

Fig.3.4: TEM image of nanoparticle of 13 nm prepared at 12.5 pH.

Magnetite power was characterized on X-ray diffractometer, Phillips make PW 1800 X'pert pro model with wide angle range from 6^o to 80^o as shown in Fig 3.5, Fig 3.6, Fig 3.7 and Fig 3.8 with their respective particle sizes. The size of the crystal is calculated by Scherrer's formula and the XRD wavelength of 0.15406 nm was used for characterization as well as k was taken as 0.89 depends upon crystal used.

Scherrer's formula:

$D = K\lambda / (B\cos\theta)$

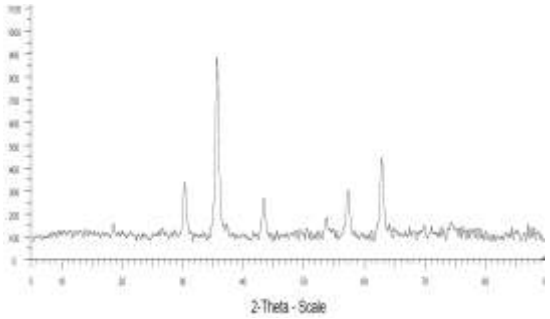

Fig.3.5: XRD Pattern of Fe_3O_4 nanoparticle of 27.6 nm (8 pH). X-axis: 2 Theta, Y-axis: Intensity

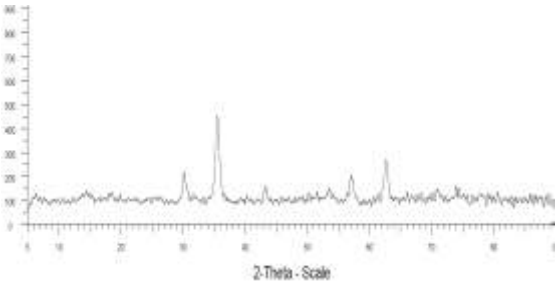

Fig.3.6: XRD Pattern of Fe_3O_4 nanoparticle of 23.7 nm (10 pH). X-axis: 2 Theta, Y-axis: Intensity

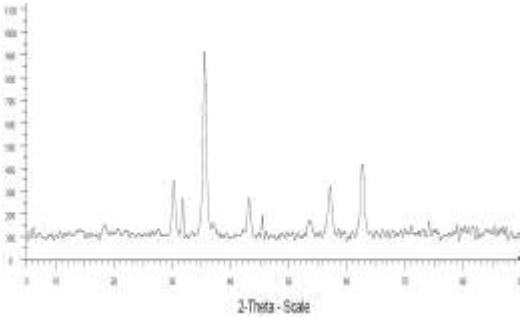

Fig.3.7: XRD Pattern of Fe_3O_4 nanoparticle of 19 nm (11.5 pH). X-axis: 2 Theta, Y-axis: Intensity

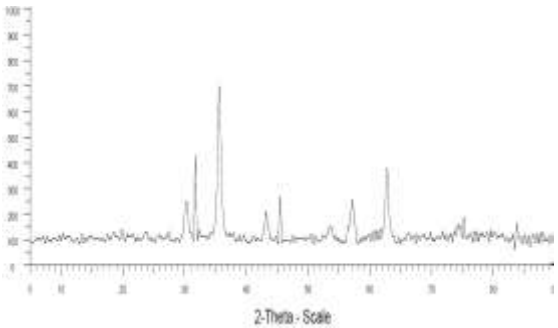

Fig.3.8: XRD Pattern of Fe_3O_4 nanoparticle of 12.7 nm (12.5 pH). X-axis: 2 Theta, Y-axis: Intensity

Table no.3.1 shows the diameters of nanoparticles obtained by TEM and XRD prepared under 8 pH, 10 pH, 11.5 pH, 12.5 pH further saturation magnetization is listed as observed.

Tableno.3.1

pH	8	10	11.5	12.5
D_{TEM} (nm)	30	24	19	13
D_{XRD} (nm)	27.6	23.7	18.7	12.7
M_{sat} (emu/gm)	88.0	86.9	79.0	78.9

IV. EXPERIMENTAL METHODS

4.1 Functional Block Diagram

Fig.4.1 shows the basic functional block diagram of measurement of volumetric concentration.

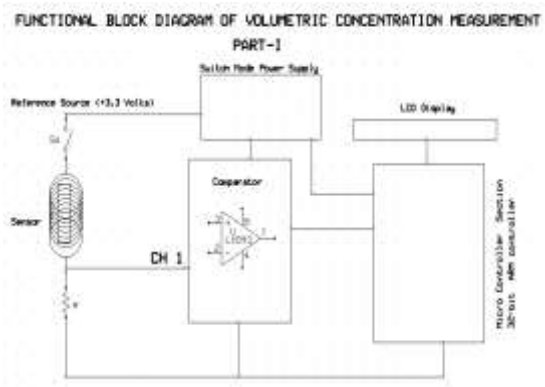

Fig.4.1 Functional block diagram of measurement of volumetric concentration

In order to measure Volumetric concentration, a magnetic sensor is used. Sample of magnetic fluid is placed in the core of magnetic sensor. The value of magnetic sensor, which is inductance, varied according to volumetric concentration of sample. Sensor contributes to L-R transient circuit which forms the basic principle behind the measurement of volumetric concentration. This transient circuit is connected to CH-1 of comparator section. The inductance value of the sensor increased with higher value of volumetric concentration of the sample and in turn, increased the time constant (L/R) of this transient circuit. This increased variation in time constant has given proportionate variation in pulse counts by microcontroller. This was evaluated with the volume concentration and displayed on LCD, having 2 lines and 16 characters per line. The comparator is used to compare the exponential rise in the potential across sensing resistor in L-R circuit and compared with a reference potential of 2.5 Volts obtained from temperature compensated band-gap potential reference. This obtained output level of comparator was given to microcontroller's input GPIO pin to control the pulses to be counted according to the state of GPIO pin. Table 4.1 shows the physical parameters of the sensor.

Table no.4.1 Sensor parameters

Parameters	Values
Processor clock	60MHz
Number of turns (N)	16000
Length of coil (l)	7 cm
Diameter of solenoid (D)	5 cm
Resistance (R)	3.3KΩ
Time constant ($\tau = \frac{L}{R}$)	$2.73*10^{-3}$ sec

To obtain an unknown Volumetric concentration of the sample, internal data processing was carried out on standard samples with data interpolation technique. The famous Newton-Gregory formula was not used here due to the fact that, the interpolation is best at end of the data table. Here sample data may lie anywhere in the table. Therefore, Stirling's approximation is proper here as this approximation is an average of Gauss forward difference and backward difference analysis. The value of unknown or measured sample was determined by interpolating measured data with standard table by applying Stirling's approximation.

Table no.4.2 Count vs. % volumetric concentration for particle size 30nm

Sr No.	%VC	Count
1	0	113377
2	0.25	118776
3	0.5	124775
4	0.75	130174
5	1	136173
6	1.25	142012
7	1.5	147570

Table no.4.3 Count vs. % volumetric concentration for particle size 24nm

Sr No.	%VC	Count
1	0	113377
2	0.25	118240
3	0.5	122790
4	0.75	127436
5	1	132990
6	1.25	137995
7	1.5	142977

Table no.4.4 Count vs. % volumetric concentration for particle size 13nm

Sr No.	%VC	Count
1	0	113377
2	0.25	117100
3	0.5	120306
4	0.75	122910
5	1	125714
6	1.25	128701
7	1.5	131710

Table no.4.5 Count vs. % volumetric concentration for particle size 11.8nm

Sr No.	%VC	Count
1	0	113377
2	0.25	115965
3	0.5	118239
4	0.75	120512
5	1	122786
6	1.25	125060
7	1.5	127334

.

Fig. 4.2 shows the variation of count with respect to percentage of volumetric concentration at 300 K for particle sizes of 30 nm, 24 nm, 13 nm, 11.8 nm. It can be observed from this graph, that count increases with an increase in the percentage of volumetric concentration. For smaller diameters, the counts are observed to be higher than that for larger diameters.

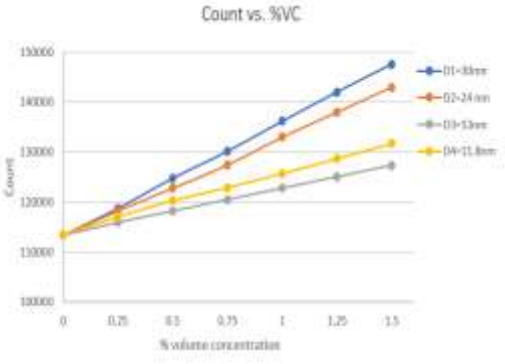

Fig 4.2 Count vs. % volumetric concentration for particle sizes 30 nm, 24 nm, 13 nm, 11.8 nm.

Table no.4.6 Count vs. particle size with % VC- 0%

Sr No.	Particle Size (nm)	Count
1	11.8	11337
2	13	11337
3	24	11337
4	30	11337

Table no.4.7 Count vs. particle size with % VC- 0.25%

Sr No.	Particle Size (nm)	Count
1	11.8	11596
2	13	11710
3	24	11823
4	30	11877

Table no.4.8 Count vs. particle size with % VC- 0.50%

Sr No.	Particle Size (nm)	Count
1	11.8	11823
2	13	12051
3	24	12278
4	30	12477

Table no.4.9 Count vs. particle size with % VC- 0.75%

Sr No.	Particle Size (nm)	Count
1	30	12051
2	24	12392
3	13	12733
4	11.8	13017

Table no.4.10 Count vs. particle size with % VC- 1.00%

Sr No.	Particle Size (nm)	Count
1	11.8	12278
2	13	12733
3	24	13188
4	30	13617

Table no.4.11 Count vs. particle size with % VC- 1.25%

Sr No.	Particle Size (nm)	Count
1	11.8	12506
2	13	13074
3	24	13642
4	30	14217

Table no.4.12 Count vs. particle size with % VC- 1.50%

Sr No.	Particle Size (nm)	Count
1	11.8	12733
2	13	13415
3	24	14097
4	30	14757

Fig. 4.3 shows the variation of count with respect to particle sizes at 300 K for percentage of volumetric concentrations of 0%, 0.25%, 0.50%, 0.75%, 1%, 1.25% and 1.50%. From this graph, it can be observed that, count decreases with increasing particle sizes. For higher values of volumetric concentrations (%), the counts are observed to be higher than that for lower volumetric concentrations (%).

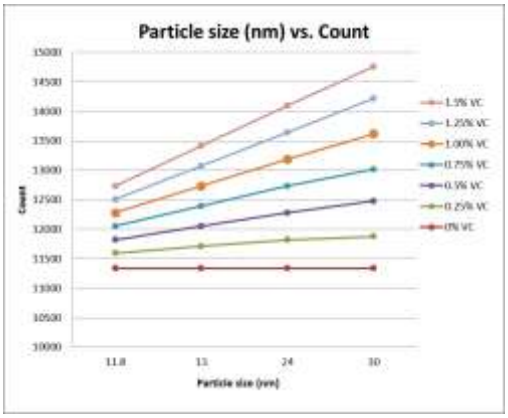

Fig 4.3. Count vs. particle size for different percentage of volumetric concentrations of 0%, 0.25%, 0.50%, 0.75%, 1%, 1.25% and 1.50%.

Table no.4.13 Thermal conductivity vs. % volumetric concentration for particle size 30nm

Sr No.	% VC	K (mW/m*K)
1	0	136
2	0.02	144
3	0.04	154
4	0.06	164
5	0.08	172
6	0.1	182
7	0.12	190
8	0.14	197
9	0.16	203
10	0.18	210
11	0.2	217
12	0.22	223
13	0.24	228

Table no.4.14 Thermal conductivity vs. % volumetric concentration for particle size 24nm

Sr No.	% VC	K (mW/m*K)
1	0	136
2	0.02	140
3	0.04	148
4	0.06	156
5	0.08	164
6	0.1	170
7	0.12	177
8	0.14	184
9	0.16	192
10	0.18	199
11	0.2	204
12	0.22	209
13	0.24	215

Table no.4.15 Thermal conductivity vs. % volumetric concentration for particle size 13nm

Sr No.	% VC	K (mW/m*K)
1	0	136
2	0.02	140
3	0.04	144
4	0.06	150
5	0.08	155
6	0.1	161
7	0.12	168
8	0.14	173
9	0.16	177
10	0.18	181
11	0.2	185
12	0.22	189
13	0.24	195

Table no.4.16 Thermal conductivity vs. % volumetric concentration for particle size 11.8nm

Sr No.	% VC	K (mW/m*K)
1	0	136
2	0.02	138
3	0.04	141
4	0.06	145
5	0.08	150
6	0.1	156
7	0.12	161
8	0.14	166
9	0.16	170
10	0.18	174
11	0.2	178
12	0.22	182
13	0.24	186

Fig. 4.4 shows the variation of thermal conductivity K (mW/ m-k) with the variation of percentage volumetric concentration at 300 K for particle sizes 30 nm, 24 nm, 13 nm, 11.8 nm. From this graph, it can be observed that, count increases with increasing particle sizes. For higher values of particle size, the thermal conductivity is observed to be higher than that for smaller particle sizes.

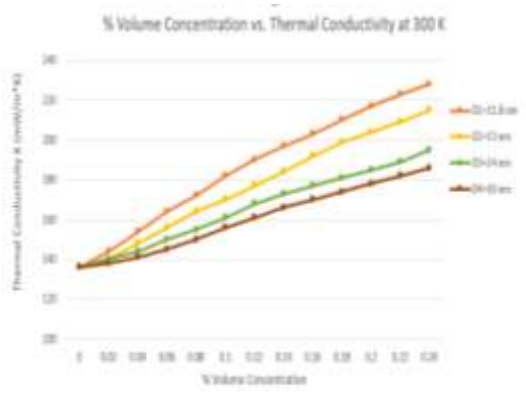

Fig 4.4 Percentage of volume concentration vs. thermal conductivity K (mK/ m-k) for diameters of 11.8 nm, 13 nm, 24 nm, 30 nm.

V. RESULTS AND DISCUSSION

Table no. 4.2, 4.3, 4.4 and 4.5 shows variation of count with variation in percentage volumetric concentration for particle size of 30 nm, 24nm, 13nm, 11.8nm respectively and graph was plotted and shown in fig 4.2. Measurement was carried out at 300 K. It is observed from this graph that counts were increasing with an increase in the percentage volumetric concentration. For larger diameters, the counts are observed to be higher than that for smaller diameters**.**

Table no. 4.6, 4.7, 4.8, 4.9, 4.10, 4.11, 4.12 shows variation of count with variation in particle size (nm) for 0%, 0.25%, 0.50%, 0.75%, 1.00%, 1.25% and 1.50% volumetric concentrations respectively and a graph was plotted and shown in fig 4.3. Fig 4.3 shows the variation of count with respect to particle sizes at 300 K for percentage of volumetric concentrations in the order of 0%, 0.25%, 0.50%, 0.75%, 1%, 1.25% and 1.50%. It can be observed from the graph that the counts increase with increasing particle sizes. For higher values of volumetric concentrations, the counts are observed to be higher.

Table no. 4.13, 4.14, 4.15 and 4.16 shows the variations in thermal conductivity K (mW/m-k) with variations in volumetric concentration for the particle size of 30 nm, 24 nm, 13 nm and 11.8 nm. Fig.4.4 shows consolidated graphs of the variations in thermal conductivity K (mW/m-k) with the variations in volumetric concentration at 300 K for particle sizes 30 nm, 24 nm, 13 nm, 11.8 nm. From this graph, it can be observed that for smaller particle sizes, thermal conductivity is higher and varies proportionately with volumetric concentration.

VI. CONCLUSION

6.1It was observed from the graph that the counts increase with increasing particle sizes. For higher values of volumetric concentrations, the counts are observed to be higher. This is due to the fact, that the saturation magnetization of higher size particles is higher. Therefore, the permeability of core at sensor increases and in turn increases the inductance value of sensor. This gives rise to more L/R time constant and more number of counts thereafter.

6.2 It was also observed that for smaller particle sizes, thermal conductivity is higher and varies proportionately with volumetric concentration. This effect was attributed to the increasing order of total surface area of all the particles taken together in the order in which the particle sizes were going low.

REFERENCES

Journal Papers:

[1] S. D. Kemkar, Milind Vaidya, Dipak Pinjari, Chandrakant Holkar, Sanjana Kemkar, Siddhesh Nanaware, Sanjukta Kemkar, Energy Conversion on Differential Magnetization of Fe_3O_4 ferrofluid, Int. Journal of Engineering Research and Application, Vol. 7, Issue 1, (Part-3), January 2017, pp.01-10.

[2] S. D. Kemkar, Milind Vaidya, Dipak Pinjari, Sammit Karekar, Sanjana Kemkar, Siddhesh Nanaware, Sanjukta Kemkar, Application of mixed colloidal magnetic fluid in single domain Fe_3O_4 and $NiFe_2O_4$ ferrite nanoparticles in audio speakers, Int. Journal of Engineering Research and Application, Vol. 7, Issue 1, (Part-3), January 2017, pp.11-18.

[3] Kinnari Parekh & R V Upadhyay, Characterization of transformer oil based magnetic fluid, Indian Journal of Engineering & Material Sciences, vol. 11, Aug. 2004, pp. 262-266

[4] Jong-Chun Lee and Woo-Young Kim, "Experimental study on the dielectric breakdown voltage of the insulating oil mixed with magnetic nanoparticles," Physics Procedia 32 (2012), pp. 327-334

[5] Cristina STAN, Constantine P. CRISTESCU, Maria BALASOIU, N. PEROV, V. N. DUGINOV, T. N. MAMEDOV, L. FETISOV, Investigations of a Fe_3O_4-Ferrofluid at different temperatures by means of magnetic measurements, U. P. B. Sci. Bull., Series A, Vol. 73, Iss. 3, 2011, 117-124

[6] M. Timko, P. Kopcansky, L. Tomco, K. Marton, M. Koneracka, F. Herchl and N. Tomasovicova, DC and AC dielectric properties transformer oil based magnetic

fluid, NSTI- Nanotech 2009, Vol. 1, 2009, 190-193.
[7] P. Kopcansky, K. Marton, L. Tomco, M. Koneracka, M. Timko, I. Potocova, F. Herchl.
[8] Innocent Nkurikiyimfura, Yanmin Wang, Zhidong Pan, Heat transfer enhancement by magnetic nanofluids- A review, Renewable and Sustainable Energy Review 21 (2013), 548-561.
[9] M.S. Dababneh, N.Y. Ayoub, I. Odeh and N.M. Laham, "Viscosity, resistivity and surface tension measurements of Fe,O, ferrofluid," Journal of Magnetism and Magnetic Materials, 125 (1993), pp. 34-38.
[10] A. Ryskin, II Pleiner, Influence of a Magnetic Field on the Soret Effect dominated Thermal Convection in Ferrofluids, Phys. Rev. E. 69 (2004).
[11] M. I. Shliomis, M. Souhar, Self-Oscillatory Convection caused by the Soret Effect, Europhys. Lett. EPL. 49 (2000), 55-61.
[12] M. Krichler, S.Odenbach, Thermal conductivity measurements on ferrofluids with special reference to measuring arrangement, Journal of Magnetism and Magnetic Materials 326 (2013) 85-90.
[13] E. Blums, New problems of particle transfer in ferrocolloids: Magnetic Soret effect and thermoosmosis, Eur. Phys. J. E 15, 271-276 (2004).
[14] K. I. Morozov, Thermal Nonequilibrium Phenomena in Fluid Mixtures, Lect. Notes Phys., Vol. 584, edited by W. Kohler, S. Wiegand (Springer, Berlin, 2002) pp. 38.
[15] S. N. Semenov, Colloid J. 59,488 (1997).
[16] S D Kemkar, Milind Vaidya, Deepak Pinjari, Anand Jadhav, Sanjana Kemkar, Siddhesh Nanaware, Sanjukta Kemkar, DC Conductivity Study of Ferrofluid of Fe_3O_4 Ferrite Nanoparticles Dispersed in Hydrocarbon Carrier, International Journal of Innovative Research in Science, Engineering and Technology, Vol. 6, Issue 1, January 2017, pp. 962-987.

Proceedings Papers:

[17] S D Kemkar, H S Mahajan, M Vaidya, Ferrofluid based optical fiber switch, AIP conference proceedings 2012, Vol-1447,512-522
[18] S D Kemkar, 2-D Fractional Micro controller based tilt measurement system using ferrofluid, 13th National Seminar on Physics and Technology of Sensors March 3-5, 2008, C-8-1.

Books:

[19] Rosensweigh R E, Ferrohydrodynamics, Cambridge University Press, Cambridge, 1986.

Sanjay Kemkar "Evaluation of Volumetric Concentration of Ferrofluid Useful For Heat Extraction in High Power Transformers "International Journal of Engineering Research and Applications (IJERA) , vol. 8, no.6, 2018, pp.38-45